A Cryogenic Quantum-Based RF Source

J. A. Brevik[1,#], A. S. Boaventura[1,2], M. A. Castellanos-Beltran[1], C. A. Donnelly[1], N. E. Flowers-Jacobs[1], A. E. Fox[1], P. F. Hopkins[1], P. D. Dresselhaus[1], D. F. Williams[1], S. P. Benz[1]

[1]National Institute of Standards and Technology, Boulder, CO 80305 USA

[2]University of Colorado, Boulder, CO 80305 USA

[#]justus.brevik@nist.gov

***Abstract*— We performed a preliminary calibrated measurement of the output power of a Josephson arbitrary waveform synthesizer up to 1 GHz. We present the results and measurement procedure for generating quantum-based signals using an array of Josephson junctions operating at cryogenic temperature and calibrating those signals to transfer the on-wafer quantum-based accuracy to room temperature.**

***Keywords*— Josephson arrays, quantization, signal synthesis, standards, superconducting integrated circuits, voltage measurement, power measurement, digital-analog conversion.**

I. Introduction

The Josephson arbitrary waveform synthesizer (JAWS) has been demonstrated to be an invaluable tool for synthesizing quantum-based voltage signals for metrology in the audio-frequency range [1]. Our goal is to extend the metrology capability of the JAWS system as a quantum-based source to the radio-frequency range. Our initial effort has extended the maximum waveform synthesis frequency to several gigahertz, while our goal is to eventually increase it to tens then hundreds of gigahertz [2].

The synthesis of arbitrary waveforms using pulse-driven Josephson junctions (JJs) is detailed in [1],[3]. Briefly, waveforms are encoded into a pattern of return-to-zero pulses with two or more levels using a delta-sigma modulation algorithm that modulates the separation of the pulses. The output patterns have calculable spectra with high spurious-free dynamic range (SFDR) and signal-to-noise ratio (SNR) near the fundamental synthesis frequency, despite the large digitization error resulting from the limited number of encoded pulse levels. When this pulse pattern is generated by a standard room-temperature digital-to-analog converter (DAC), the output signal will fluctuate with time and environmental conditions and will have degraded SFDR and SNR compared to the calculated spectrum. The signal from this DAC output can be conditioned by an array of JJs, which acts as a pulse quantizer. The resulting signal is stable, has an amplitude with quantum-based accuracy, and a spectrum that has exceptionally high SFDR and SNR.

Under the proper conditions, when a JJ is biased using a current pulse it will generate a quantized voltage pulse with an integrated time area that is exactly equal to a multiple of a magnetic flux quantum $\Phi_0 = h/2e$, where h is the Planck constant and e is the elementary unit of electric charge. Through this effect, an array of JJs can be used to generate quantized output pulses that have stable and invariant time-integrated area based on quantum effects and tied to fundamental constants.

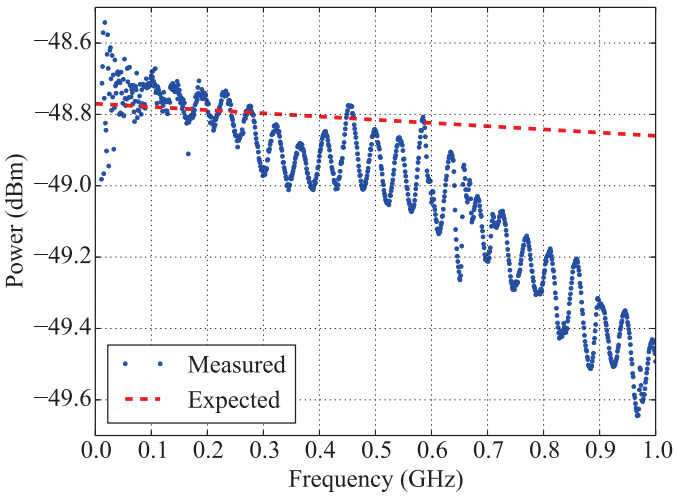

Fig. 1. The calibrated output power versus synthesis frequency for the JAWS system (dots) and the expected frequency-dependent value (dashed line).

Unique to JJ circuits, the quantized pulses are generated over a range of bias current amplitude and other conditions called the quantum locking range (QLR). When the JAWS system operates within its QLR, every incident bias pulse is transformed by every JJ in the array into a quantized output voltage pulse. This ensures that the output amplitudes of the synthesized waveforms are quantum-based, stable, independent of operating location, and immune to small variations in operating bias, temperature and other conditions.

JAWS systems have synthesized waveforms up to 1 GHz, but those signals were not corrected for the errors occurring between the JJ devices and the room-temperature measurement [4]. In this work, we used a cryogenic probe station to measure the output signals of a JAWS circuit and a set of cryogenic calibration standards to reference the signals measured at room temperature to the signals generated on chip, where they have quantum-based accuracy [5],[6].

II. Experimental Setup

As a first step in demonstrating the quantum-based output of the JAWS system, we have measured and corrected its output power versus synthesis frequency (frequency response) up to 1 GHz, as shown in Fig. 1. The goal of the experiment was to demonstrate that the frequency response could be

978-1-7281-0951-0/20/$31.00 ©2020 IEEE

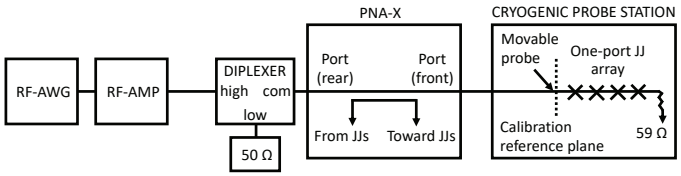

Fig. 2. Block diagram of the measurement setup.

generated and properly corrected so that it is in agreement with the expected value and independent of the synthesis frequency, within the limits discussed in section III-C. Calibrated phase measurements of the JAWS output signals will be included in future experiments.

A schematic representation of the measurement setup is shown in Fig. 2. The main equipment used in the experiment includes a cryogenic probe station with a cryogenic chip containing the JJ circuit and standards, a Keysight N5242A precision network analyzer (PNA-X), and a Keysight M8195A 65 gigasample-per-second arbitrary waveform generator (RF-AWG)[1]. The RF-AWG was used to apply the current bias pulses to the JJ array, and an RF amplifier was used to increase their amplitude. The bias signal was transmitted to the high-frequency port of a diplexer with a 5 GHz crossover frequency. The low-frequency port of the diplexer was terminated with a 50 Ω resistor, and the common port was connected to the rear-panel input to one port of the PNA-X. The front panel of that port was connected to a movable cryogenic microwave probe via a feedthrough port on the probe station.

The current bias pulse signal contains a component at the fundamental synthesis frequency that drives the distributed inductance of the JJ array coplanar waveguide (CPW), creating a frequency-dependent voltage error that adds vectorially to the desired signal [3]. The diplexer was used to high-pass filter the current bias pulses and reduce this so-called "feedthrough" error. However, the high-pass port presented a high impedance to the low-frequency synthesized (<5 GHz) signal traveling from the JJ array toward the PNA-X. To limit the reflection of the synthesized signal from the high-pass port, a diplexer was used instead of a high-pass filter so that a $50\ \Omega$ termination was presented to the JJ output signal.

We used a PNA-X to measure the signals from the JJ array and to measure the calibration standards. Only one port of the PNA-X was used for the JJ device measurement, but two ports were used during the on-chip calibration standard measurements. The PNA-X port that was connected to the JJ circuit includes an internal bias tee, which was used to apply an additional dc bias current to the bias pulse pattern when the QLR was measured. A comb generator, triggered by a 10 MHz square wave generated by a synchronized channel of the RF-AWG, was used as a phase reference for the PNA-X.

[1]Commercial instruments are identified in order to adequately specify the experimental procedure. Such identification does not imply recommendation or endorsement by NIST, nor does it imply that the equipment identified is necessarily the best available for the purpose.

For this first experimental iteration, we measured a one-port JAWS circuit, as shown in Fig. 2. In this circuit, the JJs are embedded in a CPW in 500 vertical stacks with three JJs per stack, for a total of 1500 junctions [7]. One end of the CPW is connected to the ground plane via a termination resistor with a design impedance of $50\ \Omega$ to absorb the residual bias pulse signal. The opposite end of the CPW has contact pads to accept a microwave probe that was used to apply the bias signals and measure the JJ output signal. This circuit topology provides roughly half of the full signal of the quantized output pulses generated by the JJ array, as explained in section III-C.

A set of calibration standards were fabricated in niobium on the same chip as the JAWS circuit. These superconducting calibration standards provide the basis for the second-tier calibration of the PNA-X down to the wafer reference plane. They include a multi-line ("thru"-reflect-line) TRL kit with five line standards ranging in length from $70\ \mu\mathrm{m}$ to $9\ \mathrm{mm}$, and several short, thru, open, and load standards. Additional details about the calibration kit can be found in [6].

We used a cryogenic probe station to measure the signals generated by the JAWS circuit and to perform the cryogenic calibration of those signals. The chip containing the cryogenic standards and JJ device was mounted on a cryogenic stage that was controlled at 4 K. The cryogenic probe station has two microwave probes that can each be controlled along three axes of motion using cryogenic piezoelectric nanopositioners. The microwave probes were used to measure the complex voltage waveforms traveling toward and away from the device under test, and one probe was also used to apply the bias signals to the JJ array. An optical microscope was used to image the 4 K stage through transparent windows in the cryostat jacket and radiation shields to position the probes on the cryogenic chip.

III. Measurement

A. Measurement Procedure

We measured the frequency response of the JAWS output signal by measuring the power at the fundamental of single output tones that were synthesized in steps of 1 MHz from 10 MHz to 1 GHz. These 991 single-tone bipolar waveforms were each encoded into a bias pulse pattern with a minimum of 10 000 waveform periods using a second-order, three-level $[-1, 0, +1]$, bandpass delta-sigma modulator at a 64 gigasample-per-second rate. To reduce the signal at the fundamental in the bias pulse pattern and decrease the feedthrough error, the three-level codes were transformed to five-level codes so that each bias pulse had bracketing half-amplitude pulses and each pulse block had effectively zero average current [3]. For this experiment, quantum-locked operation could be achieved across the entire synthesis frequency range only by reducing the amplitude of the waveforms to 2.5 % of the full scale possible with the given sample rate. The limitation on the mark density of the pulses is under investigation, but an increase in the signal amplitude should be possible in future measurements.

We performed the measurement by sequentially programming each of the 991 pulse patterns into the RF-AWG, setting the PNA-X measurement frequency to the corresponding value of the synthesis frequency, and measuring the forward and backward complex waveforms at the input of the JJ circuit. During these measurements the dc offset bias was set to zero and the cryostat windows were closed.

B. Calibration

After measuring the JAWS signals, we performed the calibration measurements that were used to correct the raw frequency response data. The calibration procedure is described in detail in [5],[6], but a brief description of the procedure follows. We measured the on-chip cryogenic standards on a 991-point frequency grid matching the single-tone synthesis values. To establish the second-tier calibration reference plane at the end of the microwave probes, we used both probes and PNA-X ports to measure the two-port cryogenic TRL standards. Next, we disconnected the PNA-X coaxial cables from the probe station and performed a short-open-load-thru (SOLT) calibration at the end of the cables to determine the first-tier calibration reference plane. We then calibrated the absolute amplitude using a power meter that is traceable to the NIST calorimeter power reference, and calibrated the absolute phase using a frequency comb generator that is traceable to the NIST electro-optic sampling system. We used the NIST microwave uncertainty framework (MUF) software to compute the error correction [8], which we then used to correct the JJ signal measurements to produce the frequency response shown in Fig. 1. The uncertainty for the correction has not yet been calculated.

C. Expected Signal Level

When generating quantum-based JAWS signals, the exact dc value of the quantized pulse area across the JJ array is calculable. There are several additional effects that must be considered when calculating the expected output signal level, especially at higher frequencies, that are discussed below. The calculable dc signal level—assuming the pulses are ideal delta functions and synchronized—depends on the number of JJs in the array, the maximum density of pulses, and the number of quantized pulses generated for each input bias pulse. The codes used in this experiment were all designed for a -42 dBm output signal.

Because we measured a one-port JJ device in this experiment, only a portion of each quantized output pulse area was collected and an additional correction to the calculable signal level is required. As detailed in [9], the quantized output pulses split with a portion propagating along the CPW in the direction of the bias pulses and the other portion traveling in the opposite direction. The ratio of the split is determined by the voltage division of the impedances seen in either direction from the point of generation. The measured dc impedance of the nominally 50 Ω termination resistor was 59 Ω, and the measured dc impedance at the probe looking toward the PNA-X was 50 Ω. Therefore, approximately 46 % of the quantized pulse area was measured, reducing the total power by -6.8 dB to a total expected dc power level of ~ -48.8 dBm.

The quantized pulses are not perfect delta functions but have a finite pulse width that causes the signal level to decrease at higher synthesis frequencies. There are two main contributions to the finite pulse width. The first is simply due to the finite characteristic frequency (~ 20 GHz) of our JJs, which we expect to reduce the signal by -0.06 dB at 1 GHz [4]. The second effect relates to pulse propagation. Due to the finite distribution of the JJs along the CPW, the sum of the quantized pulses that propagate in the same direction as the incident bias signal has a narrower overall pulse shape than the summed pulse traveling in the opposite direction. Since a one-port circuit was used in this work, we measured the broader composite pulses. Given 500 JJ stacks at the standard 6.5 μm stack spacing, the estimated output power reduction is -0.8 % or -0.03 dB at 1 GHz [9]. These two pulse width effects have negligible impact on the total expected power at 10 MHz, but reduce it by -0.09 dB to around -48.9 dBm at 1 GHz. There is a corresponding negative slope in the expected frequency response between 10 MHz and 1 GHz of -0.09 dB, which is a 2.1 % error in power. This error can be reduced in the future by increasing the characteristic frequency of the JJs.

In previous measurements, the contribution of the feedthrough error was considerable, especially at 1 GHz [4]. In this experiment, the feedthrough was effectively eliminated by the improved filtering provided by the stop-band of the high-pass diplexer filter. The feedthrough error was reduced below the noise floor of the PNA-X for even a 1 Hz measurement bandwidth, setting its upper limit at -120 dBm at 1 GHz.

D. Verification of Quantum Locking Range

It is critical that the system operates within the QLR of the JJ circuit at each synthesis frequency step to ensure that the output power at the fundamental synthesis tone is quantum-based and constant, within the limits described in the previous section. We verified the QLR for each of the 991 synthesis steps by measuring the JAWS output with respect to a dc offset current applied to the JJ array. As the magnitude of the dc offset increases from zero, the JJs will eventually either fail to emit a quantized output pulse for each bias pulse or will emit more quantized pulses than intended, thus defining the boundaries of the QLR. When this boundary is crossed, there is little change in the output power at the fundamental. However, any omission or addition of pulses in the quantized pattern will cause the noise floor of the calculable output spectrum near the fundamental to change in an appreciable way.

We measured the QLR by stepping an offset current bias applied to the array and recording the power at the 50 noise spurs above and the 50 spurs below the fundamental synthesis tone that make up the calculable noise floor. The PNA-X was configured for 10 Hz bandwidth and 101 measurement points on a frequency grid that captured the synthesis tone and the 100 nearest noise spurs. The power was recorded for each

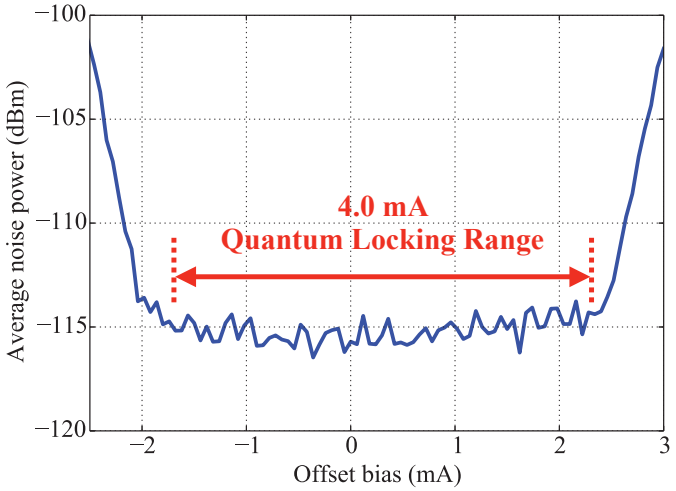

Fig. 3. Characteristic measurement of the quantum locking range (QLR) with respect to offset bias current for a single synthesis frequency step (300 MHz). The average power of the noise floor near the synthesis tone is plotted against the offset bias current. The dashed lines indicate the boundaries of the 4.0 mA QLR measured for this synthesis frequency step.

of the 101 frequency points while stepping the offset bias from -3 mA to +3 mA. The average of the power for the 100 noise spurs was then plotted against the offset bias as in Fig. 3, which shows a characteristic QLR measurement for a single-tone synthesis step. An inflection point occurs where the average noise power starts to increase with the bias offset, corresponding to the boundaries of the QLR. The span in current from the negative to positive inflection points was calculated for each synthesis frequency. We measured a minimum QLR of 3.8 mA across the entire synthesis range, demonstrating the output of the JAWS source was measured while in quantum-locked operation.

E. Calibrated Frequency Response

The resulting calibrated frequency response is shown in Fig. 1, along with the calculated frequency-dependent power from section III-C. At low frequency there is reasonable agreement between the measured and expected values. However, as the synthesis frequency increases, the measured value drops further below the expected value and we observe an excess frequency-dependent "roll-off." In addition, the response shows a ripple with roughly 0.2 dB peak-to-peak amplitude. The maximum deviation in the measured power from the expected frequency-dependent value occurs at 967 MHz, where the measured power is -49.6 dBm. This error is equivalent to about -0.8 dB or 17 % in power.

The source of the additional roll-off is under investigation. It is possible that we have underestimated the width of the quantized output pulses and therefore have underestimated the expected roll-off. We plan to make calibrated measurements of the widths of the input bias and quantized output pulses at the wafer reference plane to re-evaluate our estimate. The origin of the ripple is also under investigation, and we should be able to remove it in future measurements.

IV. Conclusion

We have produced a preliminary calibrated measurement of the frequency response of the output power of a JAWS circuit up to 1 GHz. The calibrated output power differs by a maximum of -0.8 dB, or 17 % in power, from the expected value. This large deviation is due to a combination of ripple and excess roll-off of the signal at higher synthesis frequencies. The latter contribution is the dominant source of error, and we attribute it to a larger than expected quantized pulse width. This will be mitigated in the future by optimizing the bias pulses and by increasing the characteristic frequency of the JJs. The output power is currently about -49 dBm, but we should be able to increase this to -30 dBm, which is the level where the source becomes most useful for RF metrology. We can do so by transitioning to two-port device measurements, by increasing the encoded signal amplitudes, and by increasing the number of JJs in the array. Finally, we plan on estimating the uncertainty of the calibration procedure in our next measurement campaign and including it in our error analysis.

Acknowledgment

The authors thank the NIST Boulder Microfabrication Facility. The authors also thank Adam Sirois for his work on the cryogenic probe station. This research was supported by NIST's Innovations in Measurement Science program. This work is a contribution of the U.S. Government and is not subject to U.S. copyright.

References

[1] S. P. Benz and C. A. Hamilton, "A pulse-driven programmable Josephson voltage standard," *Applied Physics Letters*, vol. 68, no. 22, pp. 3171–3173, 1996.

[2] P. F. Hopkins, J. A. Brevik, M. Castellanos-Beltran, C. A. Donnelly, N. E. Flowers-Jacobs, A. E. Fox, D. Olaya, P. D. Dresselhaus, and S. P. Benz, "RF waveform synthesizers with quantum-based voltage accuracy for communications metrology," *IEEE Transactions on Applied Superconductivity*, vol. 29, no. 5, pp. 1–5, Aug 2019.

[3] J. A. Brevik, N. E. Flowers-Jacobs, A. E. Fox, E. B. Golden, P. D. Dresselhaus, and S. P. Benz, "Josephson arbitrary waveform synthesis with multilevel pulse biasing," *IEEE Transactions on Applied Superconductivity*, vol. 27, no. 3, pp. 1–7, April 2017.

[4] C. A. Donnelly, N. E. Flowers-Jacobs, J. A. Brevik, A. E. Fox, P. D. Dresselhaus, P. F. Hopkins, and S. P. Benz, "1 GHz waveform synthesis with Josephson junction arrays," *IEEE Transactions on Applied Superconductivity*, vol. 30, no. 3, pp. 1–11, April 2020.

[5] A. S. Boaventura, J. A. Brevik, D. F. Williams, A. E. Fox, P. F. Hopkins, P. D. Dresselhaus, and S. P. Benz, "Calibrating a quantum-based radio-frequency source," *ARFTG 2020*, submitted for publication.

[6] A. S. Boaventura, D. F. Williams, R. A. Chamberlin, J. G. Cheron, A. E. Fox, P. D. Dresselhaus, P. F. Hopkins, I. W. Haygood, and S. P. Benz, "Microwave modeling and characterization of superconductive circuits for quantum voltage standard applications at 4 K," *IEEE Transactions on Applied Superconductivity*, vol. 30, no. 2, pp. 1–7, March 2020.

[7] B. Baek, P. D. Dresselhaus, and S. P. Benz, "Co-sputtered amorphous Nb_x Si_{1-x} barriers for Josephson-junction circuits," *IEEE Transactions on Applied Superconductivity*, vol. 16, no. 4, pp. 1966–1970, Dec 2006.

[8] www.nist.gov/services-resources/software/wafer-calibration-software.

[9] C. A. Donnelly, J. A. Brevik, N. E. Flowers-Jacobs, A. E. Fox, P. D. Dresselhaus, P. F. Hopkins, and S. P. Benz, "Quantized pulse propagation in Josephson junction arrays," *IEEE Transactions on Applied Superconductivity*, vol. 30, no. 3, pp. 1–8, April 2020.